

We regret that some of the pages in the microfiche copy of this report may not be up to the proper legibility standards, even though the best possible copy was used for preparing the master fiche.

AAEC/E461



INIS  
AU7904040  
AAEC/E461

**AUSTRALIAN ATOMIC ENERGY COMMISSION  
RESEARCH ESTABLISHMENT  
LUCAS HEIGHTS**

**APPLICATION OF THE MONTE CARLO TRANSPORT CODE MORSE  
TO THE CALCULATION OF PULSED NEUTRON EXPERIMENTS**

by

**M.T. RAINBOW**

March 1978

ISBN 0 642 59664 6

AUSTRALIAN ATOMIC ENERGY COMMISSION  
RESEARCH ESTABLISHMENT  
LUCAS HEIGHTS

APPLICATION OF THE MONTE CARLO TRANSPORT CODE MORSE  
TO THE CALCULATION OF PULSED NEUTRON EXPERIMENTS

by

M.T. RAINBOW

ABSTRACT

An accurate calculation tool is essential for the assessment of nuclear data by the pulsed neutron technique. The Monte Carlo transport code MORSE is such a tool and its application to the calculation of pulsed neutron experiments is presented. Modifications to the code and a set of ancillary programs to enable the direct comparison of calculation with experiment are described.

The time profile of the pulsed neutron source is treated in a manner which allows more efficient use of the code. However, as a consequence some parameters, such as detector responses at different times, are no longer uncorrelated. Error analysis which takes proper account of these correlations is presented.

National Library of Australia card number and ISBN 0 642 59664 6

The following descriptors have been selected from the INIS Thesaurus to describe the subject content of this report for information retrieval purposes. For further details please refer to IAEA-INIS-12 (INIS: Manual for Indexing) and IAEA-INIS-13 (INIS: Thesaurus) published in Vienna by the International Atomic Energy Agency.

NEUTRON TRANSPORT; PULSED NEUTRON TECHNIQUES; COMPUTER CALCULATIONS;  
M CODES; NEUTRON TRANSPORT THEORY; MONTE CARLO METHOD; NEUTRON BEAMS

## CONTENTS

	Page
1. INTRODUCTION	1
2. THE MORSE CODE	3
2.1 The Neutron Source	5
2.2 Detectors (Boundary Crossing Estimators)	6
2.3 Stop/Restart Feature	6
2.4 Double-precision Accumulators	7
3. MORSE CALCULATIONS	8
3.1 Folding MORSE Output	9
3.2 Time-dependent Detector Reaction Rates	10
3.3 Time-dependent Spectra	12
3.4 Calculation of Adjoint Flux?	13
4. SUMMARY	15
5. ACKNOWLEDGEMENTS	15
6. REFERENCES	16
Figure 1 Method of generating random $x_i$ , which are distributed according to a given probability density function $f(x)$	17
Figure 2 Unfolded and folded $^{235}\text{U}$ fission rates in a depleted uranium assembly as calculated by MORSE	18
Figure 3 Logarithmic derivatives, $\lambda(t)$ , of $^{235}\text{U}$ fission rates in a depleted uranium assembly	19
Figure 4 Results of polynomial fits to the log of the $^{235}\text{U}$ fission rate over the time interval 25.76 to 38.08 ns	20
Figure 5 Results of polynomial fits to the log of the $^{235}\text{U}$ fission rate over the time interval 41.44 to 53.76 ns	21
Figure 6 Angle integrated spectrum for the 2.3 MeV $^9\text{Be}(d,n)^{10}\text{B}$ reaction	22
Figure 7 Unfolded and folded neutron energy spectra in a depleted uranium assembly as calculated by MORSE	23
Figure 8 More unfolded and folded neutron energy spectra in a depleted uranium assembly as calculated by MORSE	24
Figure 9 Source pulse profile used to generate the folded spectra presented in Figures 7 and 8	25
Figure 10 Evolution of the neutron spectra in a depleted uranium assembly as calculated by MORSE	26

## 1. INTRODUCTION

The pulsed neutron technique, applied as a diagnostic tool to heavy metal assemblies, is based on the observation that as neutrons slow down in such assemblies they do so with little dispersion of the energy spectrum. As a result, the behaviour of the neutron population (measured as a detector response) at any particular time reflects the nuclear properties of the assembly material in some particular energy range. For a typical source spectrum of mean energy  $\sim 2$  MeV, the neutron population slows down to a mean energy of  $\sim 100$  keV in  $\sim 100$  ns. Thus, a measurement of the time behaviour of such a neutron population in a heavy metal assembly, over the time range 0 to 100 ns, probes an energy region of considerable interest in the neutronics of fast reactors, and can be used as a means of assessing cross section data on international nuclear data files.

In essence, the technique consists of:

- (i) measuring a time-dependent detector response in an assembly following the injection of a pulse of neutrons into the assembly, and
- (ii) calculating the same time-dependent response using the data to be evaluated.

Any inconsistencies between calculation and measurement can be attributed to inadequacies in the nuclear data used to describe the nuclear characteristics of the material in the assembly.

Such a strategy assumes that the calculational method can account accurately for details of the neutron interactions in the assembly. Until recently, the only calculational tool available was the zero-dimensional diffusion code TENDS [Maher *et al.* 1967; Moo *et al.* 1974]. This code was developed for use with large volume pulsed thermal systems in which the neutron distribution is separable in space, energy and time during the time range of interest - a situation in which the application of a zero-dimensional code is valid. The diffusion theory calculation produced results which were in excellent agreement with experiment when the nuclear data used were modified to take proper account of the physical properties of the material used in the experimental assembly [Ritchie 1968]. Excellent agreement was also obtained with experimental results for small polycrystalline pulsed assemblies in which space-energy-time separability and the assumptions of diffusion theory do not strictly

apply [Ritchie *et al.* 1970]. This is in line with the general experience that diffusion theory 'works' in many situations in which it is not strictly applicable.

In pulsed heavy metal assemblies, the neutron distribution is a continuously slowing down distribution and is certainly not separable in space, energy and time. This is similar to the case for small polycrystalline assemblies in which the neutron distribution is also a slowing down distribution. The success of the zero-dimensional diffusion code in the latter case suggested that the code might also be applicable to experiments with heavy metal assemblies.

Experiments with heavy metal assemblies have to be performed in such a way as to allow a spatial Fourier decomposition of measured time-dependent detector responses to yield essentially space-independent results for direct comparison with the results of TENDS calculations. The parameter used for comparison was the logarithmic derivative of the detector reaction rate associated with the fundamental Fourier spatial mode. The agreement between theory and experiment [Moo *et al* 1974; Rainbow & Ritchie 1975] was not satisfactory. This was particularly so in the time range immediately after the pulse, when the neutron energy spectrum is in the range 0.5 to 5.0 MeV, where the data for inelastic scattering, which is the dominant interaction, are least certain and the approximations of diffusion theory are least likely to hold. In the absence of any other calculational tool, it was not possible to assess quantitatively the extent to which the calculational method was at fault.

The combinatorial geometry version of the multigroup Monte Carlo radiation transport code MORSE [Emmett 1975] has been acquired from the Oak Ridge National Laboratory. This code is able to treat, in detail, the geometry of the experiment and should, in principle, be an accurate calculational method.

The present report describes the application of the MORSE code to the calculation of pulsed neutron experiments. Modifications to the input, output and data accumulation subroutines are discussed, and a set of ancillary programs, which have been produced to facilitate the comparison of experiment with calculation, are also described.

A feature of the method is that the MORSE calculations are done with a source time profile having a narrow (short duration) rectangular form. Time-dependent detector reaction rates, or time-dependent spectra

suitable for comparison with experiment, are synthesised by convoluting the code output with a histogram representation of the experimental source pulse profile. As a result, if a particular experiment is repeated and a different source pulse profile pertains, a new MORSE calculation is not required.

A disadvantage of Monte Carlo calculations is that they require long periods of computer time, but this handicap is offset in the present application by the considerable reduction in experimental complexity and effort, quite apart from the essential feature of its intrinsic accuracy. Experiments conducted to allow a spatial Fourier decomposition take a long time (several days) to perform and, because the same source must apply for measurements made at different spatial positions to satisfy normalisation requirements, they are very demanding on the long-term stability of the experimental equipment, particularly the pulsed neutron source. As a result, the frequency of aborted measurements of this type was quite high. The availability of a code such as MORSE, which is able to account for all important aspects of an experiment, obviates the need for Fourier decomposition and requires the measurement of a time-dependent detector reaction rate only at a single position. Such a measurement takes a couple of hours. In addition, since there is no normalisation requirement, minor instabilities of the pulsed source are integrated into both the measured source pulse profile and the measured detector reaction rate and, as a result, are of no consequence.

## 2. THE MORSE CODE

The MORSE code is a multipurpose, multigroup Monte Carlo neutron and gamma-ray transport code which can be used for a wide range of problems. Its many useful features include:

- . The ability to treat the transport of either neutrons or gamma-rays or a coupled neutron and secondary gamma-ray problem.
- . The use of multigroup cross sections.
- . The treatment of anisotropic scattering.
- . The three-dimensional combinatorial geometry package.
- . The ability to treat time-dependence.
- . The option of several types of importance sampling (e.g. Russian roulette, splitting).

The flow of the code consists of three nested loops: one for runs; one for batches; and an innermost loop for particles (neutrons or gamma-rays). A batch is processed by following the histories of a number of particles. A given problem is performed by processing a number of batches of particles; this constitutes a run. The batch processing feature is used so that statistical variations between groups of particles can be determined and errors assigned to the calculated results.

The code can be considered to consist of five separate modules:

- . random walk;
- . cross section;
- . analysis;
- . combinatorial geometry; and
- . diagnostic.

*The random walk module* consists of the routines which generate source particles and follow them through their histories.

*The cross section module* consists of the routines which process the cross section information needed by the code. This module reads cross sections for media or elements in either DTF-IV [Lathrop 1965] or ANISN [Engle 1967] format, mixes cross sections for several elements to obtain media cross sections, and determines the probabilities and angles of scattering for each group to group transfer. An option is available to write the processed cross section data onto magnetic tape or disc. This avoids reading the cross section information for a subsequent run requiring the same data.

*The analysis module* consists of those routines which handle the analysis of particle interactions such as scattering events and boundary crossings. Estimating routines, usually written by the user, identify events of interest and determine some measure such as an estimate of scalar flux. Bookkeeping routines accumulate information from the estimating routines. An arbitrary number of detectors, energy-dependent response functions, energy bins, time bins and angle bins are allowed with virtually no numerical limitations other than available core storage. Analysis is in terms of:

- . uncollided and total response;
- . response as a function of energy and detector;
- . response as a function of time and detector;

- . response as a function of time, energy and detector; and
- . response as a function of angle, energy and detector.

Each of these responses may be output, if requested, along with the associated fractional standard deviations (fsd).

*The combinatorial geometry module* describes general three-dimensional material configurations in terms of unions, differences and intersections of simple bodies such as spheres, boxes, cylinders, etc. The geometry is specified by two tables. The first table describes the type and location of the set of bodies used in the geometrical description; the second identifies the physical zones in terms of unions, intersections, etc. of these bodies.

*The diagnostic module* provides an easy means of dumping, in readable format, current values of a variety of problem variables. In addition, there are numerous diagnostic error messages which may be printed by the various subroutines.

For the application of MORSE to the pulsed neutron experiment, various user subroutines have been written and several additional features incorporated in the code. These are described in the following sections.

#### 2.1 The Neutron Source

A special version of the MORSE subroutine SOURCE, which determines the initial parameters of all the source particles, has been written. Source neutrons are generated with equal probability during a finite time interval (pulse width) which is specified in the input data stream via the MORSE user subroutine INSCOR. This corresponds to a source pulse which has a rectangular time distribution.

The angle and energy dependence of the source is determined by appropriate angle-dependent source spectra read in the form of cumulative distribution functions from a local neutron source library. This library contains data for the sources used in experiments and includes the angle-dependent neutron energy spectra for the thick target  ${}^9\text{Be}(d,n){}^{10}\text{B}$  reaction measured by Whittlestone [1976, 1977] for a range of bombarding deuteron energies. Also included are some of the results of Inada et al. [1968] for the same thick target reaction. Data generated by the local code LIPNA [Ritchie 1976; Rainbow et al. 1977], which calculates angle-dependent spectra for the thick target  ${}^7\text{Li}(p,n){}^7\text{Be}$  reaction, can also be loaded into this library.

The initial parameters for each source neutron are determined by

using the random number generator package of MORSE in conjunction with the input cumulative distribution functions in the following manner. Suppose we have a parameter  $x$  (such as source neutron energy) and its probability density function  $f(x)$  as in Figure 1. The cumulative distribution function of  $x$ ,  $F(X)$ , is defined as:

$$F(X) = \int_{-\infty}^X f(t)dt \quad ; \quad 0 \leq F(X) \leq 1 \quad .$$

If the random number generator is used to generate random numbers  $\rho_i$ , where  $0 \leq \rho_i \leq 1$  and the  $\rho_i$  are independent and drawn from a uniform probability density distribution, then the  $\rho_i$  and the inverse of the cumulative distribution function  $F(X)$  may be used to generate random  $x_i$  as indicated in Figure 1. These  $x_i$  values are distributed according to  $f(x)$  [Spanier & Gelbard 1969]. At the end of each run, the accumulated source statistics are printed. They are a record of the source distribution for the calculation and may be compared with the input specifications.

## 2.2 Detectors (Boundary Crossing Estimators)

In most neutronics problems, the basic quantity of interest is a particle flux averaged over a surface. A common procedure for estimating scalar flux in Monte Carlo calculations is to score the weight of the particle divided by the absolute value of the cosine of the angle between the particle track and the normal to the detecting surface (and the area of the surface).

The MORSE subroutine BDRYX is called whenever the geometry tracking routines encounter a particle track crossing the boundary between media. It thus serves as the routine by which events of interest are identified, and the quantity of interest is estimated and passed on to the bookkeeping routines for storage in appropriate arrays.

Several versions of this routine have been written for local use. In general, the detecting surface is some section of a hollow cylinder. The neutron flux at this surface has been estimated as indicated above.

## 2.3 Stop/Restart Feature

A somewhat crude but nevertheless effective stop/restart feature has been incorporated into the code to allow long calculations to be interrupted and restarted. This is an essential feature for a code which, because it may require a large amount of core (up to 800 K bytes) and run for an extended period (tens of hours), must usually be run at

times of low demand by other computer users.

The calculation may be stopped, apart from abnormal terminations, by one or two means. The first is to complete the calculation in the normal manner by completing the requested number of runs and batches. The second is to cancel the calculation *via* the operator's console in conjunction with the local subroutine PTEST, a member of the local FORTRAN library AAE.FORTLIB. PTEST tests for a local P-type cancel command at the end of each batch. When such a command is encountered, the calculation terminates prematurely but in the normal manner, with the usual end of job printout and dump of results. In both cases, the next random number in sequence from the random number generator is stored on disc. This number may then be used as the starting random number for a subsequent restart of the calculation.

Operating a stop/restart feature in this manner means that for each separate run of the code there is a set of output data. Apart from the usual printout, which records the progress of the calculation and some of the results, each code run produces a dump of the results onto an output dataset. A program, MADD (MORSE add), has been written to combine the data from two output datasets and to write them out onto another dataset in the same form. The results on this dataset are in the same form as the results of a single calculation and, because the random number sequence has been maintained, are equivalent to those of a single extended calculation starting with the original starting random number.

#### 2.4 Double-precision Accumulators

The standard arrays which accumulate results as a MORSE calculation proceeds are in single precision. In the case of extended calculations, this can give rise to numerical problems as small quantities are added to increasingly larger quantities. To overcome this problem, a system of double-precision accumulators has been written into the code to supplement the single-precision accumulators.

A large two-dimensional array records the details of each detector event as it occurs. The contents of this array are processed every *nb* batches, where *nb* is an integer specified in the input data stream *via* the MORSE user routine INSCOR. They are sorted and then added into time-dependent response and time-dependent spectra accumulators which are stored in double precision on magnetic disc.

The code has also been arranged so that after every *mb* of these double precision transfers, there is a dump of the results onto the

output dataset. In the case of extended calculations and computer malfunctions, this serves as a means of preventing the loss of all results. The parameter mb is specified in the same way as nb.

### 3. MORSE CALCULATIONS

The MORSE code, in the modified form described above, is used to calculate two different types of pulsed neutron experiment. One of these is the integral pulsed experiment [Moo et al. 1973] in which the quantities measured are time-dependent integral detector reaction rates. The other is a pulsed experiment in which neutron energy spectra are measured as a function of time with small detectors filled with the liquid scintillator NE213 [Whittlestone 1978].

It is usual, whatever the type of experiment under consideration, for MORSE to be used to calculate the time-dependent spectrum of the neutron flux,  $\phi(\underline{x}, E, t)$ , at the detector location  $\underline{x}$ . The time-dependent reaction rate,  $R(\underline{x}, t)$ , of a detector is calculated by integrating  $\phi(\underline{x}, E, t)$  over energy  $E$  weighted by the energy response of the detector,  $\sigma(E)$ . That is

$$R(\underline{x}, t) = \int_0^{\infty} \sigma(E) \phi(\underline{x}, E, t) dE .$$

This is valid provided that:

- (a) self-shielding in the detector is negligible;
- (b) flux depression caused by the detector is negligible; and
- (c) absorption by the detector does not affect the time-dependence of the neutron flux in the experimental assembly.

This is normally the case and it allows the results of a single MORSE calculation to be used to calculate the time-dependent reaction rate of any detector of interest for which the energy response is known. If, however, these conditions do not apply, then it is necessary to include the detector explicitly in the MORSE calculation and to perform a separate calculation for each detector.

In practice, the experimenter usually does not have good control over the source pulse profile, but is able to measure it accurately. The effect of this is that during an experiment which involves the measurement of several different quantities (such as a particular detector reaction rate at several different positions or several different detector reaction rates at one position), the effective beam

pulse profile usually changes by a small but significant amount. To allow efficient use of the code, it was decided to make the MORSE calculations independent of the source pulse profile by performing them with a source pulse profile having a narrow rectangular form. As a consequence, the raw MORSE results must be folded with an experimental source pulse profile to produce results suitable for comparison with experimental results. The following sections describe how this is done, indicate its effect on the associated error analysis, present some typical results and describe a new recipe, for the parameterisation of time-dependent detector reaction rates, which has arisen as a result of pulse profile folding and its effect on error analysis.

### 3.1 Folding MORSE Output

Consider  $y_i$ ,  $i=1,N$  to be raw (unfolded) MORSE output, where  $i$  represents a particular time bin and  $N$  is the total number of time bins considered in a calculation. The  $y_i$  may be either integral detector responses or group fluxes, depending upon whether time-dependent integral detector reaction rates or time-dependent spectra are being considered. Further, let  $f_i$ ,  $i=1,n$  be the measured time profile of the neutron source pulse where  $i$  represents consecutive time intervals (see Figure 2). So long as the MORSE source pulse width and the time bin widths associated with the raw MORSE data and the source pulse profile are the same, the folded MORSE output is then derived using the following relationship:

$$V_j = \sum_{i=1}^n f_i y_{j-i+1} \quad , \quad i \leq j \quad , \quad j = 1, N \quad ,$$

where the  $V_j$  are the folded data.

It is important to observe that  $V_i$  are non-independent data. As a consequence, any error analysis associated with operations in the time domain, such as integration or curve fitting to a time response, must include a consideration of both the variances and the covariances associated with the  $V_i$ . These are given by the following expressions:

$$\sigma^2(V_j) = \sum_{i=1}^n f_i^2 \sigma^2(y_{j-i+1}) \quad i \leq j \quad ;$$

$$\text{and } \sigma^2(V_j, V_{j+m}) = \sum_{i=1}^{n-m} f_i f_{i+m} \sigma^2(y_{j-i+1}) \quad , \quad m < n \quad , \quad i \leq j \quad ;$$

$$= 0 \quad , \quad m \geq n$$

$$= \sigma^2 (y_{j+m}, y_j) \quad j, j+m = 1, N \quad ,$$

where the  $\sigma^2(y_i)$  are the variances associated with the raw MORSE data derived from a statistical analysis of the batch results.

It should be noted that it has been assumed that the errors associated with the  $f_i$  are negligible. The extension to include a consideration of these is straightforward but tedious.

### 3.2 Time-dependent Detector Reaction Rates

A plot of the unfolded and folded time-dependent responses of a  $^{235}\text{U}$  fission detector is given in Figure 2. The calculation was made for a cube of depleted uranium of side 203 mm with a thick target  $^9\text{Be}(d,n)^{10}\text{B}$  source ( $E_d = 2.3$  MeV) at the centre of the assembly. All cross sections were group-averaged; they were generated from the ENDF/B-IV library by the code SUPERTOG [Wright et al. 1969]. The source pulse profile used for the folding is also presented in Figure 2.

A well-established practice for the intercomparison of this type of data, both measured and calculated, has been to examine the time-dependence of the derivative of the reaction rate curve. This parameterisation has proved useful because the results are independent of any amplitude normalisation effects. In the past, 'instantaneous decay constants' (or logarithmic derivatives) have been evaluated on the assumption that decay curves are exponential over a short time interval. The data were fitted to the functional form  $Ae^{-\lambda t}$  ( $t$  represents time;  $A$  and  $\lambda$  are parameters) and  $\lambda$  was evaluated. All of the data points in the time responses were independent and, as long as the same recipe for finding the  $\lambda$  was applied to both experimental and calculational data, not too much consideration was given to the goodness of fit. With the advent of folded MORSE output and non-independent data, the same procedure cannot be used to fit each set of data. This has necessitated a revision of the procedure for evaluating instantaneous decay constants and a more detailed consideration of goodness of fit.

The new procedure is to obtain a good fit with a polynomial to the logarithm of the data points and to evaluate the slope of the fitted polynomial at the centre of the range of fit. The fitting program written for this purpose is able to handle polynomials up to any order. It is based on the weighted least squares fitting criterion of minimising

the weighted sum of the squares of the residuals,  $S$ , with respect to the parameters of fit,  $p_i$ , for a non-independent set of data points [Martin 1971]. In this case,  $S$  may be written in matrix notation as

$$S = \underline{R}^T \underline{W} \underline{R} ,$$

where  $\underline{R}$  is the vector of residuals,  $\underline{R}^T$  is the transpose of  $\underline{R}$  and  $\underline{W}$  is the weight matrix. The elements of  $\underline{R}$  are

$$R_i = y_i - f(x_i, p_1, \dots, p_m) ,$$

where the  $y_i$  are the data, the  $f(x_i, p_1, \dots, p_m)$  are values of the fitting function and the  $x_i$  are values of the independent variable. The weight matrix is the inverse of the variance matrix  $\underline{V}$ , the elements of which are made up of the variances and covariances associated with the  $y_i$  as follows:

$$\begin{aligned} V_{ij} &= \sigma^2(y_i) , & i = j \\ &= \sigma^2(y_i, y_j) , & i \neq j . \end{aligned}$$

In the special case of independent data  $y_i$  (e.g. experimental data), when

$$\sigma^2(y_i, y_j) = 0 , \quad i \neq j$$

the weight matrix becomes diagonal and the fitting procedure reverts to the more usual form.

Since the data to be fitted are the logarithms of the folded MORSE data,  $V_i$ , the elements of the variance matrix are not those given in Section 3.1. They are derived by using the following result from the theory of functions of random variables. The variances and covariances associated with the function  $g(x_i)$  of random variables  $x_i$  are given by

$$\sigma^2[g(x_i)] \cong [g'(\bar{x}_i)]^2 \sigma^2(x_i) ,$$

$$\text{and } \sigma^2[g(x_i), g(x_j)] \cong g'(\bar{x}_i) g'(\bar{x}_j) \sigma^2(x_i, x_j) ,$$

where the  $g'(\bar{x}_i)$  denote the first derivatives of the  $g(x_i)$  with respect to  $x_i$  evaluated at the mean values  $\bar{x}_i$  of the  $x_i$ . This result is valid provided that the function varies slowly compared with the probability density functions of the random variables  $x_i$ . Thus, for the logarithms of the folded MORSE data:

$$\begin{aligned} V_{ij} &= \sigma^2[\ln(V_i)] \cong \sigma^2(V_i)/V_i^2 , & i = j \\ &= \sigma^2[\ln(V_i), \ln(V_j)] \cong \sigma^2(V_i, V_j)/V_i V_j , & i \neq j . \end{aligned}$$

Figure 3 is a plot of the logarithmic derivatives,  $\lambda(t)$ , evaluated from the folded  $^{235}\text{U}$  time response presented in Figure 2. Each fit was made over an interval of 11 time bins (12.32 ns), the calculated  $\lambda(t)$  being assigned to the middle time bin. Successive values of  $\lambda(t)$  were obtained by advancing the interval of fit.

During this work, it was found that fitting to non-independent data can, at times, give rise to some disconcerting results. These results were quite unexpected and are presented here for the record. Figures 4 and 5 show the results of a series of fits over the two time ranges indicated in Figure 2. Figure 4 presents fits made over the time range 25.76 to 38.08 ns which covers the peak of the detector reaction rate. Figure 5 covers the time range 41.44 to 53.76 ns during which the detector reaction rate decreases monotonically. In each case, the results presented by the top rows of the figures have been obtained by using the full weight matrix. Those compared in the bottom rows have been obtained by setting all of the covariances to zero to yield a diagonal weight matrix. It should be borne in mind that in this application, the source pulse profile covers 30 time bins (33.6 ns) so that all of the points in the fitting range are strongly correlated (all elements of the weight matrix are non-zero) and there are quite a large number of degrees of freedom (dof). The folded data in Figures 4 and 5 are derived from the raw MORSE results associated with 33 and 40 time bins, respectively.

The most disconcerting results are those for the two parameter fits with the full weight matrix. They look nothing like a reasonable fit to the data in the same sense as those on the bottom rows; however, they do correspond with the minimum of the weighted sum of residuals. It can be seen that the fits improve as the number of parameters of fit (the order of the polynomial) is increased.

### 3.3 Time-dependent Spectra

Whittlestone [1978] has used an NE213 organic liquid scintillator to measure proton recoil spectra as a function of time in the pulsed depleted uranium assembly, using a 2.3 MeV thick target  $^9\text{Be}(d,n)^{10}\text{B}$  source. These will be unfolded to yield time-dependent spectra of the neutron flux integrated over a set of time windows. A MORSE calculation of this experiment has been performed. Routines have been written to fold the raw MORSE output, integrate it over the time windows and perform the associated error analysis.

Figure 6 is a plot of the angle-integrated source spectrum for the 2.3 MeV  ${}^9\text{Be}(d,n){}^{10}\text{B}$  thick target reaction. This figure shows, in the form of neutron flux per unit lethargy, the data measured by Whittlestone [1976, 1977] and the group structured spectrum used for the calculation. Below 200 keV, it has been assumed that the flux per unit energy is constant.

Figures 7 and 8 present some calculated spectra plotted as flux per unit lethargy integrated over various time windows. The spectra in the top rows are raw MORSE results which have not been folded and correspond to a steady source of duration 0.1 ns. The spectra in the bottom rows have been obtained from the raw MORSE results by folding with the source pulse profile presented in Figure 9 and by integrating over the same time windows. The pulse profile has been calculated with the functional form

$$\exp[-|t|^3/2]$$

for a full width at half maximum height of 3 ns. This is similar to the pulse profile used in the Whittlestone measurements.

From these figures, it can be seen that the folded spectra in any particular time window are harder than the corresponding non-folded spectrum, particularly at early times. This is due to the later injection of high energy neutrons from the extended source and demonstrates that it is important to know the appropriate source pulse profile.

Figure 10 presents a plot in the same frame of the unfolded spectra presented in Figures 7 and 8. It shows the evolution of the neutron energy spectrum with the passage of time and indicates the amount of dispersion. An extra spectrum has been included in this figure; it is the one which peaks at the lowest energy and corresponds to a time window from 57.0 to 151.6 ns.

#### 3.4 Calculation of Adjoint Flux?

The present application of the MORSE code corresponds to the normal or forward solution of the transport equation. In operator formalism, the equation

$$\mathcal{L}\phi(\underline{x}, E, t) = S(\underline{x}, E, t) \quad ,$$

where  $\mathcal{L}$  is the transport operator and  $S(\underline{x}, E, t)$  is the neutron source, is solved for  $\phi(\underline{x}, E, t)$ , the normal neutron flux.  $S$  is of uniform strength over a short period of time. The unfolded detector reaction rate  $y(t)$

is obtained by integrating the product of the neutron flux and the energy response function of the detector,  $\sigma(\underline{x}, E)$  over energy and the volume of the detector as follows:

$$y(t) = \iint \sigma(\underline{x}, E) \phi(\underline{x}, E, t) d\underline{x} dE \quad . \quad (1)$$

The folded detector reaction rate  $Y(t)$  suitable for direct comparison with experimental results is obtained by folding  $y(t)$  with the measured source pulse profile  $f(t)$  as follows:

$$Y(t) = \int_0^P f(\tau) y(t-\tau) d\tau \quad , \quad (2)$$

where  $P$  is the duration of the pulse. The advantage of doing the forward calculation is that, for a single calculation of  $\phi$ , as many different detector reaction rates as required may be calculated by providing the different  $\sigma(\underline{x}, E)$  and using Equation (1).

The Morse code can, as an option, be used to solve the adjoint problem. This involves solving the adjoint transport equation with the detector as the source. The equation

$$\phi^*(\underline{x}, E, t) \mathcal{L}^* = \sigma^*(\underline{x}, E, t)$$

is solved for the adjoint flux  $\phi^*(\underline{x}, E, t)$ , where  $\sigma^*(\underline{x}, E, t)$  is a source at the detector location with an energy spectrum corresponding to the energy response of the single detector of interest and of uniform strength over a short period of time. Since  $\phi^* \mathcal{L} \phi$  is a scalar for any particular time  $t$ ,

$$\sigma^* \phi = \phi^* \mathcal{L}^* \phi = (\phi^* \mathcal{L}^* \phi)^* = \phi^* \mathcal{L} \phi = \phi^* S \quad .$$

Thus, the unfolded detector reaction may be calculated as follows:

$$y(t) = \iint \phi^*(\underline{x}, E, t) S(\underline{x}, E) d\underline{x} dE \quad . \quad (3)$$

The folded detector reaction rate  $Y(t)$  may then be obtained as above (Equation 2). From Equation (3), it is clear that the advantage to be gained by calculating the adjoint flux is that, for a single calculation of  $\phi^*$ , the different reaction rates of a single detector corresponding to many different neutron source spectra may be calculated.

The normal transport equation has been solved in the present application because, initially, these calculations were undertaken for comparison with the results of integral pulsed neutron experiments in which several different detectors ( $^{235}\text{U}$ ,  $^{239}\text{Pu}$  and  $^{237}\text{Np}$  pulse fission chambers) were used. In other applications (e.g. time-dependent spectra)

in which a single detector response is of interest, more efficient use of the code might result if the adjoint flux were calculated. It is clear, from the above discussion, that the pulse profile folding and the associated error analysis are formally the same for the forward and adjoint problems.

#### 4. SUMMARY

The MORSE Monte Carlo transport code has been tailored to fit the special requirements of the pulsed neutron experiment. Double-precision spectrum accumulators and a stop/restart facility have been incorporated into the code to facilitate the performance of calculations to high accuracy.

In practice, the experimenter usually does not have good control over the source pulse profile but is able to measure it accurately. As a consequence, during an experiment which involves the measurement of several different quantities (such as a particular detector reaction rate at several different positions or several different detectors at one position), the effective beam pulse profile usually changes by a small but significant amount. A technique has therefore been developed which involves folding the results of a MORSE calculation with a measured experimental source pulse profile to produce time-dependent results which reflect the time dependence of the source used in an experiment. This allows more efficient use of Monte Carlo calculations since one such calculation can be used to produce time-dependent responses appropriate to the different source pulse profiles occurring during many separate measurements. The disadvantage is that statistical errors in parameters such as reaction rates at different times are no longer uncorrelated. The analysis codes used to process the unfolded MORSE data to provide for valid comparisons with experimental results take proper account of these correlations in the error analysis.

The inherent accuracy of the Monte Carlo method and the ability of MORSE to account for all important details of a pulsed experiment will enable more reliable assessments of nuclear data to be made by the pulsed neutron technique.

#### 5. ACKNOWLEDGEMENTS

The author is grateful to his colleagues, Dr A.I.M. Ritchie and Mr S. Whittlestone, for frequent discussions, constructive criticism and

encouragement. The author wishes also to acknowledge Dr B.E. Clancy for directing his attention to a consideration of the adjoint calculation.

## 6. REFERENCES

- Emmett, M.B. [1975] - ORNL-4972.
- Engle, W.W. Jr. [1967] - K-1693.
- Inada, T., Kawachi, K. & Hiramoto, T. [1968] - *J. Nucl. Sci. Technol.*, 5 : 22.
- Lathrop, K.D. [1965] - LA-3373.
- Maher, K.J., Rainbow, M.T. & Ritchie, A.I.M. [1967] - Proc. IAEA Symp. Neutron Thermalisation and Reactor Spectra, Vol.II, 245.
- Martin, B.R. [1971] - Statistics for Physicists. Academic Press, London.
- Moo, S.P., Rainbow, M.T. & Ritchie, A.I.M. [1973] - *J. Nucl. En.*, 27 : 753; AAEC/E254.
- Moo, S.P., Rainbow, M.T. & Ritchie, A.I.M. [1974] - *J. Phys. D: Appl. Phys.*, 7 : 2511; also AAEC/E295.
- Rainbow, M.T. & Ritchie, A.I.M. [1975] - Proc. 3rd Nat. Soviet Conf. on Neutron Physics, Vol.I, 116.
- Rainbow, M.T., Ritchie, A.I.M. & Sullivan, L. [1977] - AAEC/E424.
- Ritchie, A.I.M. [1968] - *J. Nucl. En.*, 22 : 371.
- Ritchie, A.I.M., Maher, K.J. & Trimble, G.D. [1970] - *J. Nucl. En.*, 24 : 151.
- Ritchie, A.I.M. [1976] - *J. Phys. D: Appl. Phys.*, 9 : 15; also AAEC/E359.
- Spanier, J. & Gelbard, E.M. [1969] - Monte Carlo Principles and Neutron Transport Problems. Addison-Wesley Publishing Co.
- Whittlestone, S. [1976] - AAEC/E399.
- Whittlestone, S. [1977] - *J. Phys. D: Appl. Phys.*, 10 : 1715.
- Whittlestone, S. [1978] - private communication.
- Wright, R.Q., Greene, N.M., Lucius, J.L. & Craven, C.W. Jr. [1969] - ORNL-TM-2679.

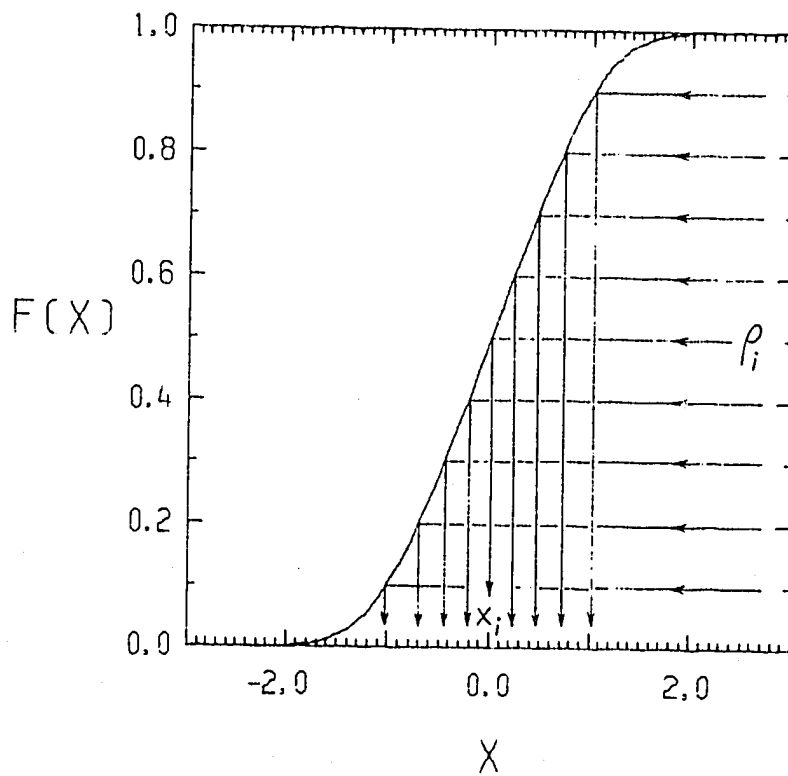
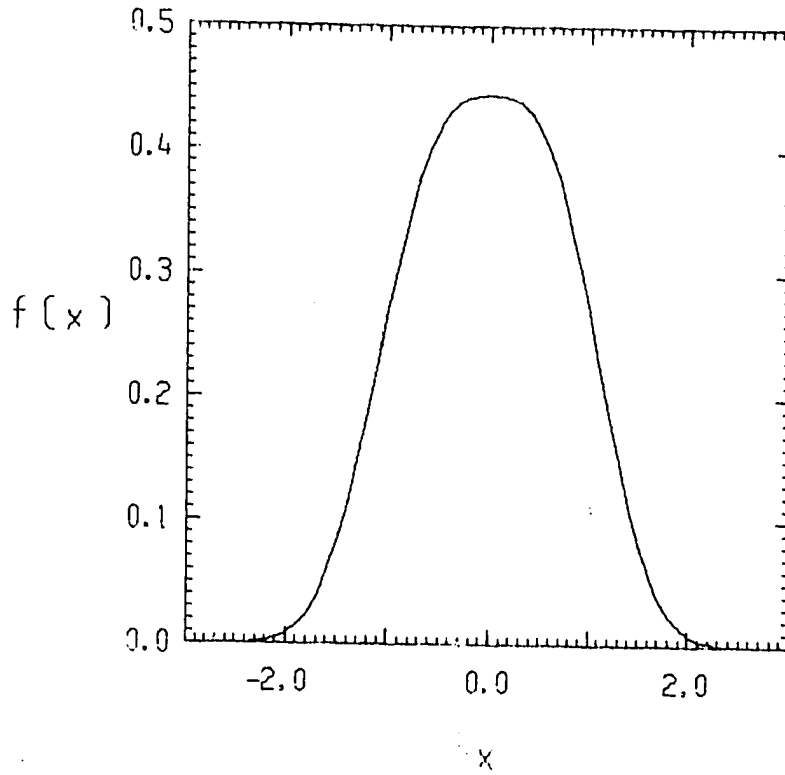


FIGURE 1. METHOD OF GENERATING RANDOM  $x_i$ , WHICH ARE DISTRIBUTED ACCORDING TO A GIVEN PROBABILITY DENSITY FUNCTION  $f(x)$

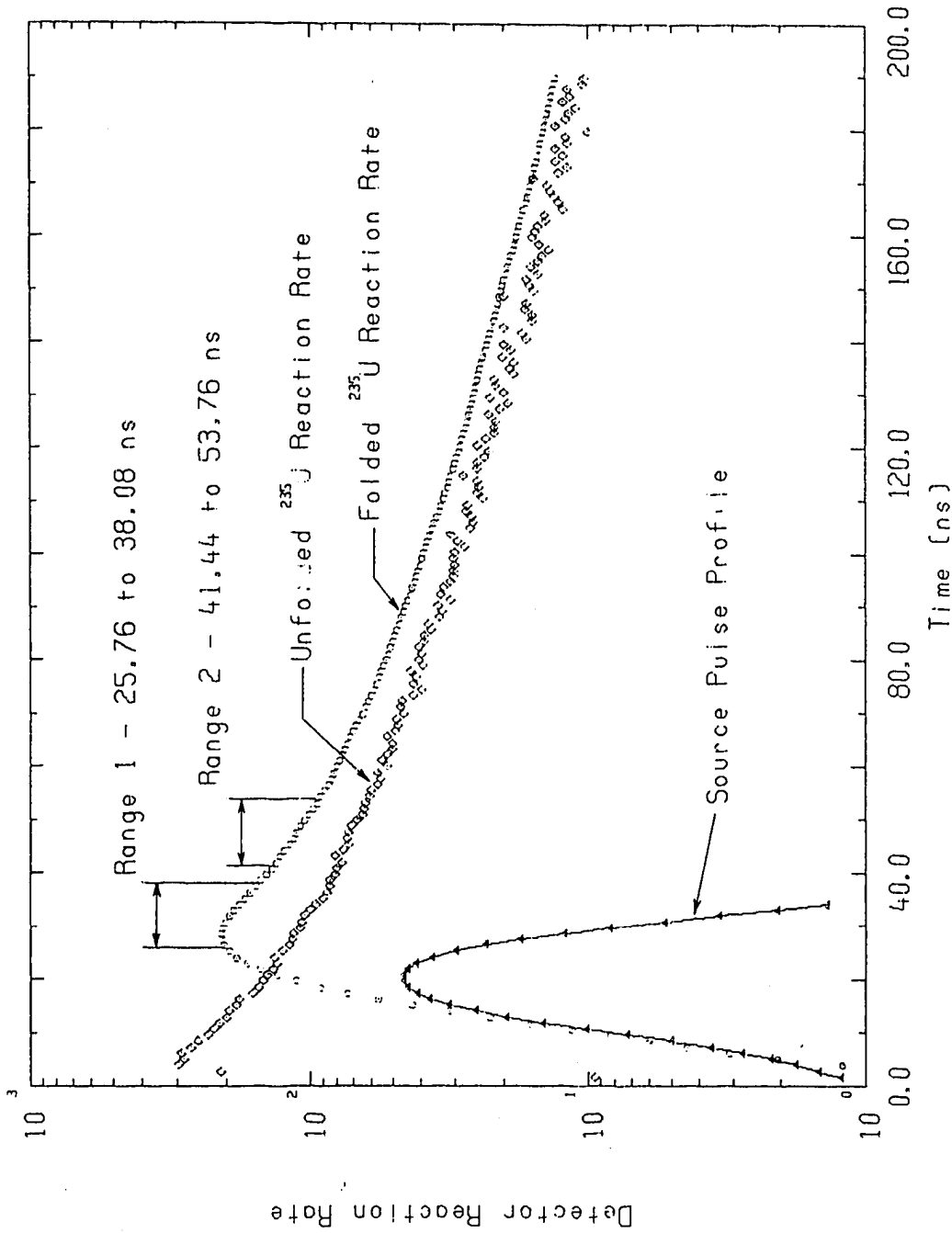


FIGURE 2. UNFOLDED AND FOLDED  $^{235}\text{U}$  FISSION RATES IN A DEPLETED URANIUM ASSEMBLY AS CALCULATED BY MORSE

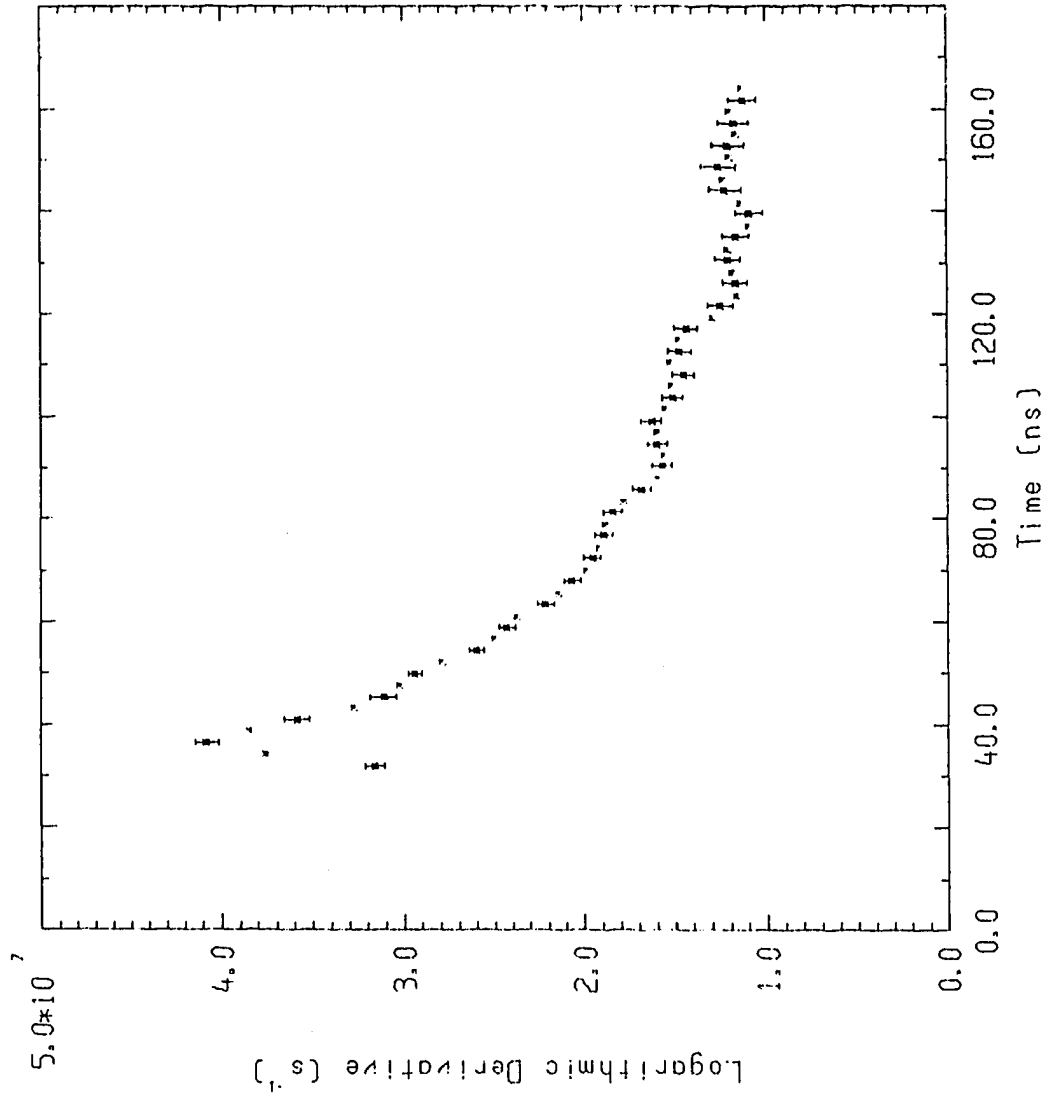


FIGURE 3. LOGARITHMIC DERIVATIVES,  $\lambda(t)$ , OF  $^{235}\text{U}$  FISSION RATES  
IN A DEPLETED URANIUM ASSEMBLY

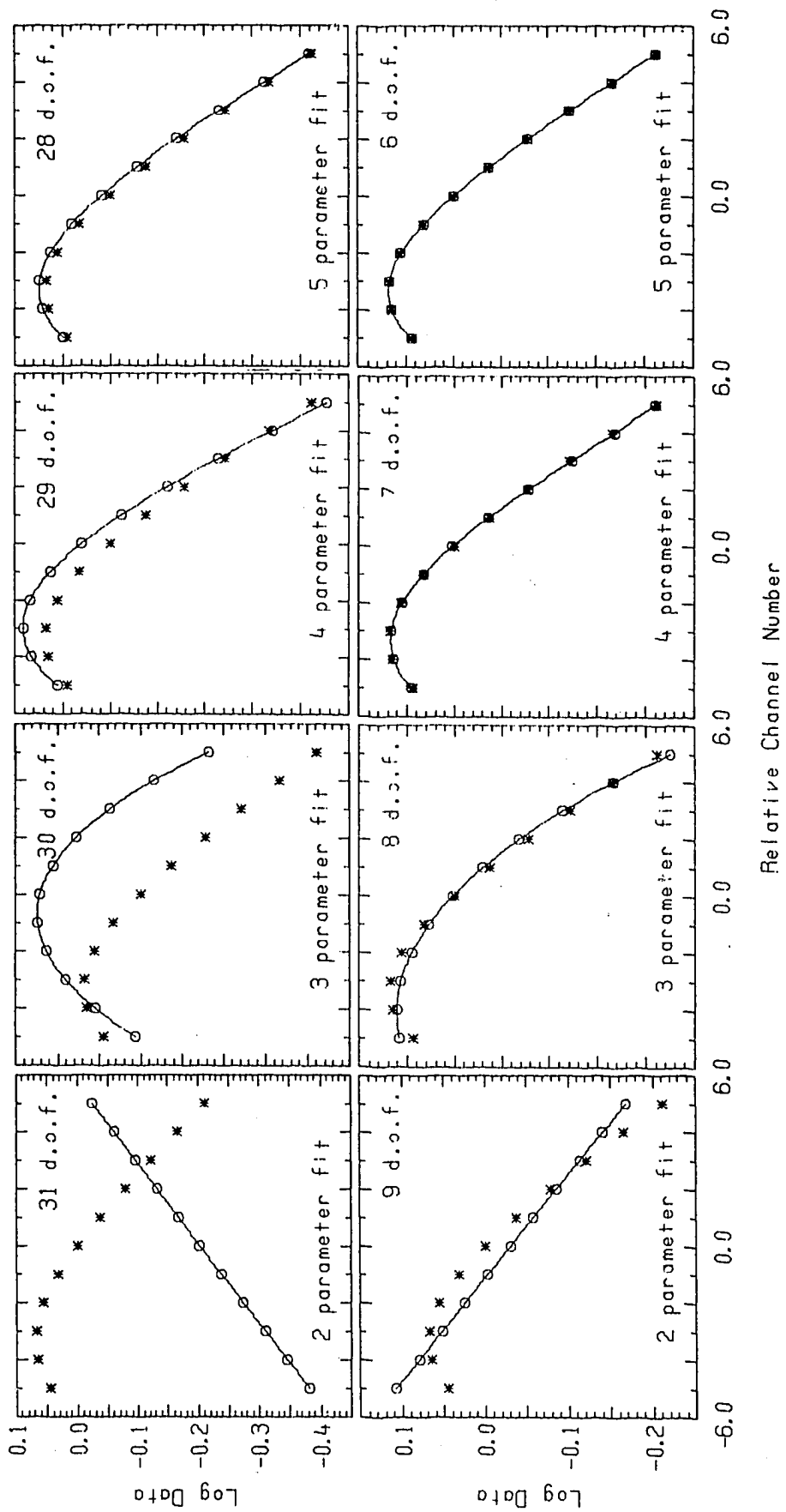


FIGURE 4. RESULTS OF POLYNOMIAL FITS TO THE LOG OF THE  $^{235}\text{U}$  FISSION RATE OVER THE TIME INTERVAL 25.76 TO 38.08 ns

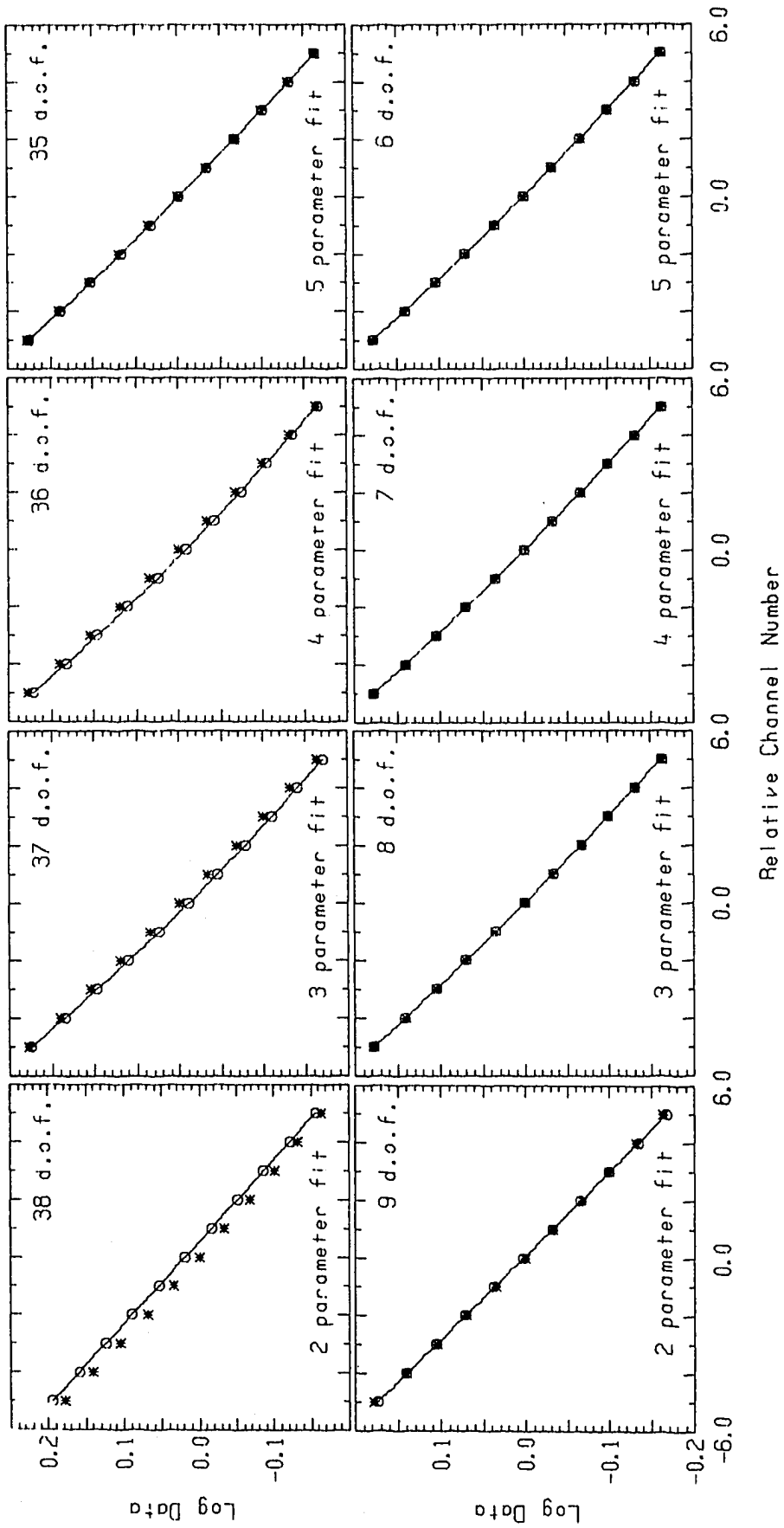


FIGURE 5. RESULTS OF POLYNOMIAL FITS TO THE LOG OF THE  $^{235}\text{U}$  FISSION RATE OVER THE TIME INTERVAL 41.44 TO 53.76 ns

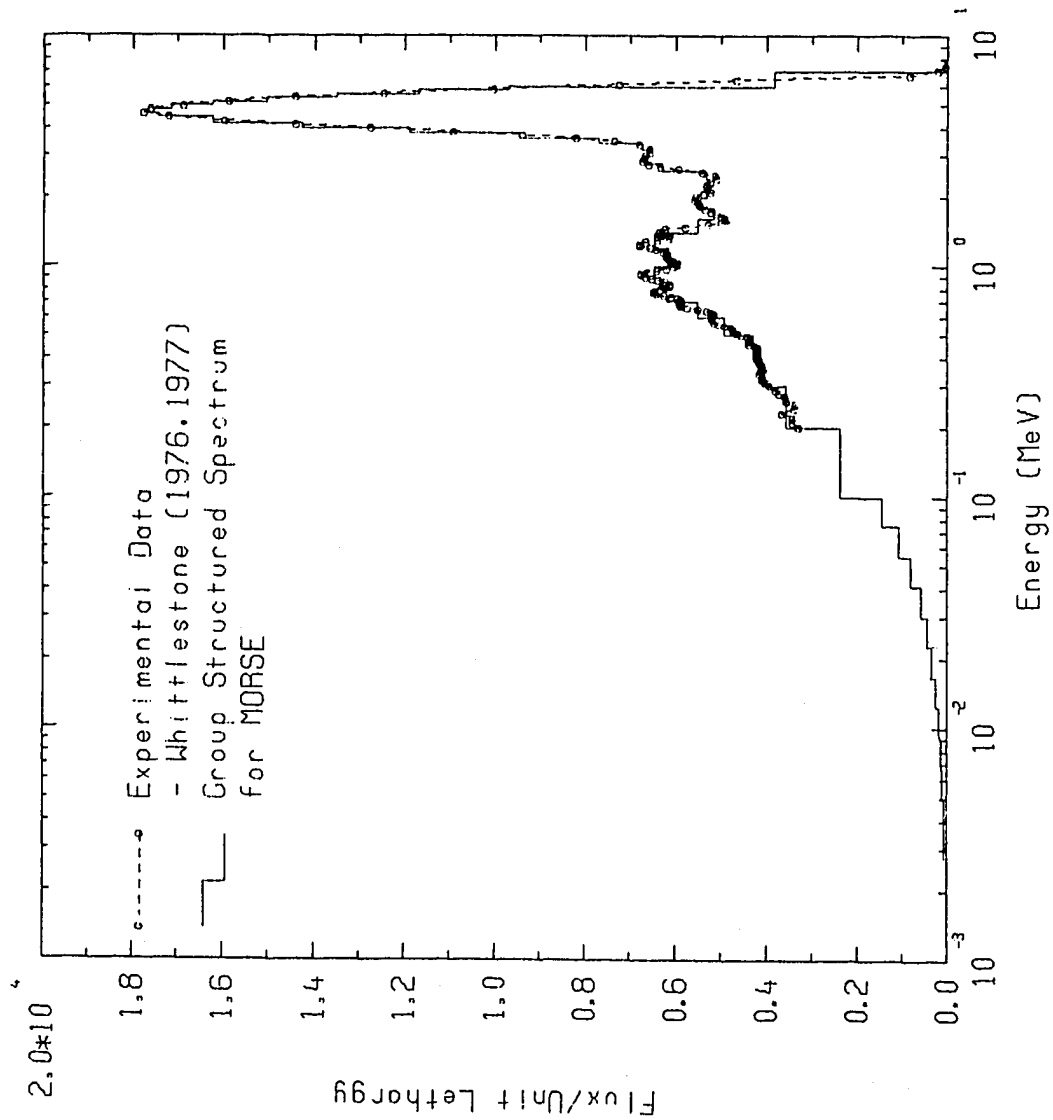


FIGURE 6. ANGLE INTEGRATED SPECTRUM FOR THE 2.3 MeV  $^9\text{Be}(d,n)^{10}\text{B}$  REACTION

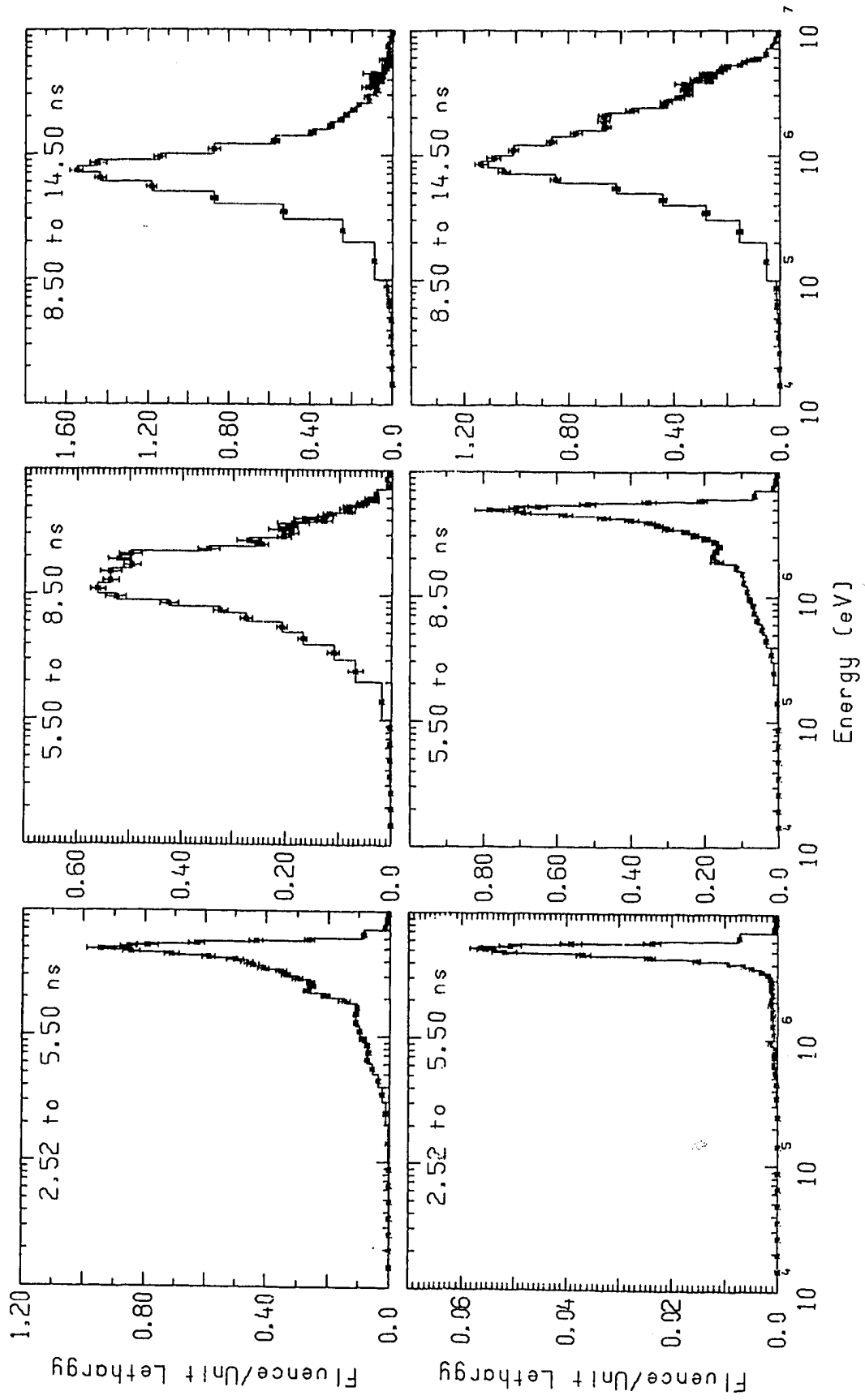


FIGURE 7. UNFOLDED AND FOLDED NEUTRON ENERGY SPECTRA IN A DEPLETED URANIUM ASSEMBLY AS CALCULATED BY MORSE

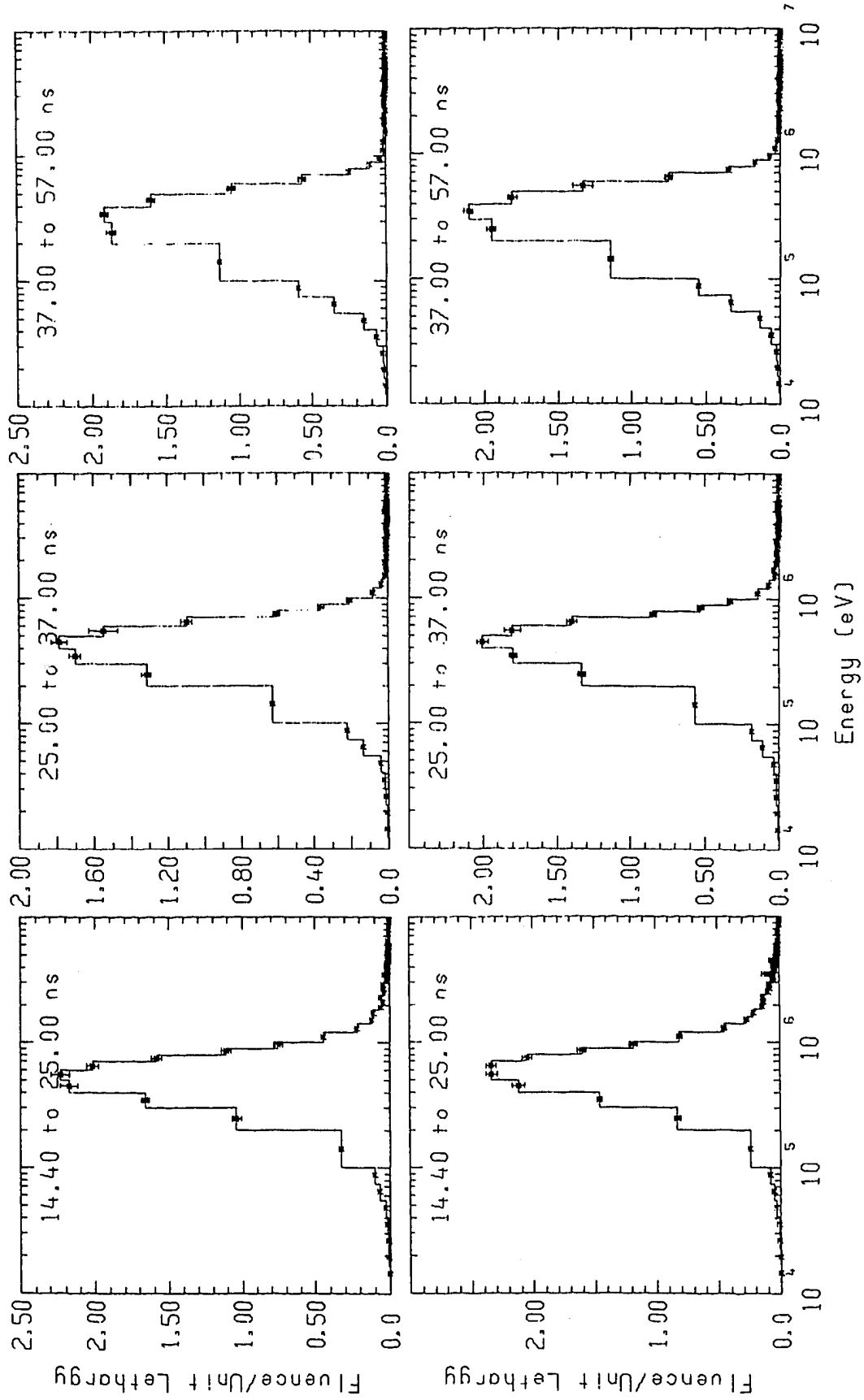


FIGURE 8. MORE UNFOLDED AND FOLDED NEUTRON ENERGY SPECTRA IN A DEPLETED URANIUM ASSEMBLY AS CALCULATED BY MORSE

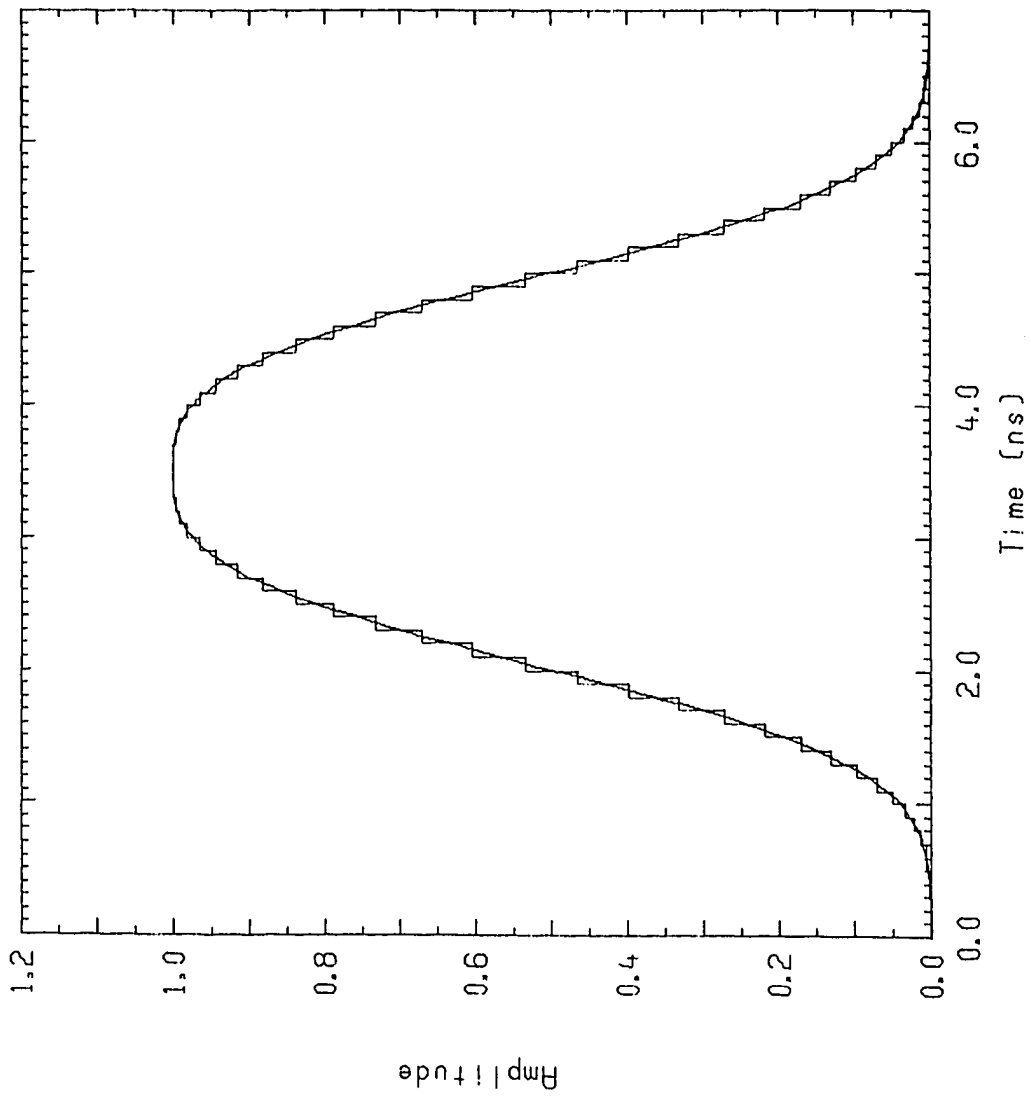
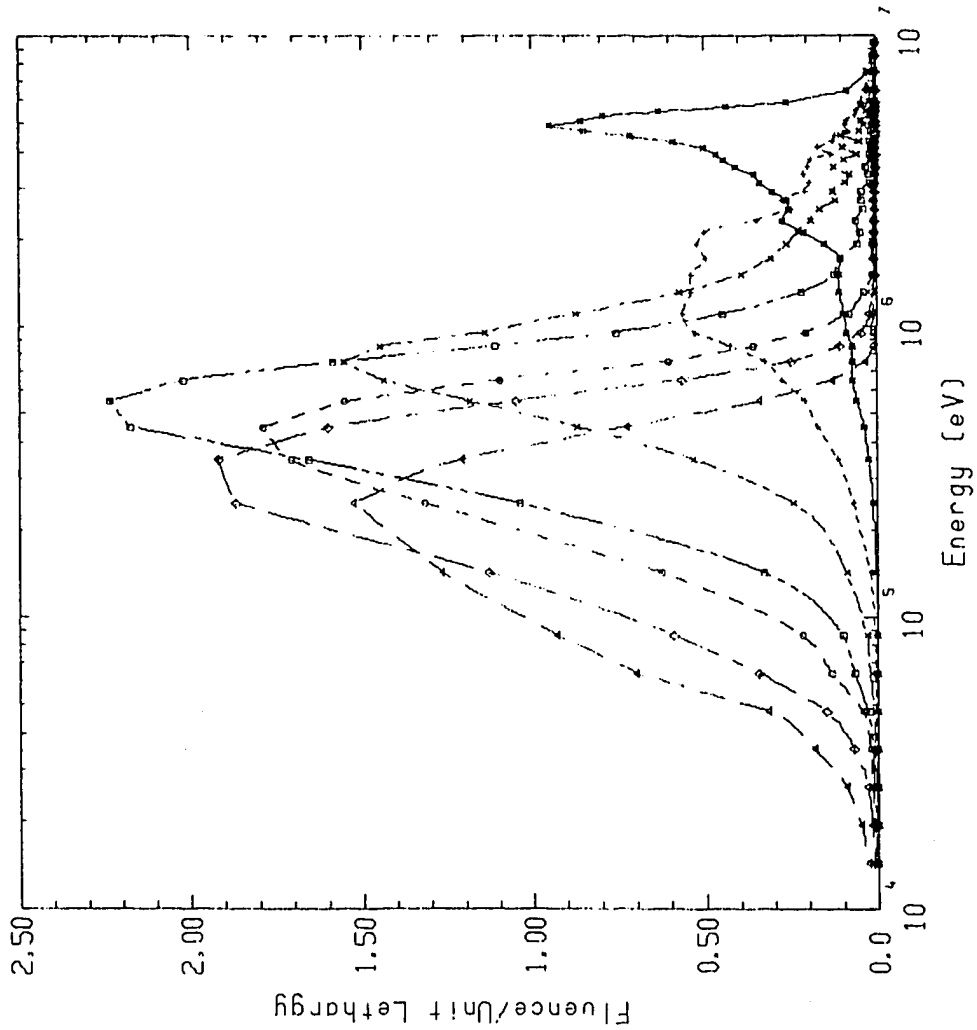


FIGURE 9. SOURCE PULSE PROFILE USED TO GENERATE THE FOLDED SPECTRA PRESENTED IN FIGURES 7 AND 8



LEGEND

- 2.52 to 5.50 ns
- - - 5.50 to 8.50 ns
- · - 8.50 to 14.50 ns
- · - 14.40 to 25.00 ns
- · - 25.00 to 37.00 ns
- · - 37.00 to 57.00 ns
- · - 57.00 to 151.60 ns

Note:

The abscissa is labelled as fluence/unit lethargy. The units are  $10^{-2}$  neutrons/cm<sup>2</sup>/unit lethargy/source neutron. This also applies to Figures 7 & 8

FIGURE 10. EVOLUTION OF THE NEUTRON SPECTRA IN A DEPLETED URANIUM ASSEMBLY AS CALCULATED BY MORSE



**B-883**



**79.10.01**